

The Energy-Autocorrelation Function in Magnetized and Unmagnetized Strongly Coupled Plasmas

T. Ott^{1*}, Z. Donkó², and M. Bonitz¹

¹ Christian-Albrechts-University Kiel, Institute for Theoretical Physics and Astrophysics, Leibnizstraße 15, 24098 Kiel, Germany

² Institute for Solid State Physics and Optics, Wigner Research Centre for Physics, H-1525 Budapest, P.O.B 49, Hungary

Received 29 October 2015, accepted 18 December 2015

Published online 25 April 2016

Key words Heat conductivity, strong coupling.

The energy-autocorrelation function is calculated for a screened Coulomb system in equilibrium and the contributions of different energy transport channels to the total heat conductivity are explored for magnetized and unmagnetized systems. A special focus is on the time scales of the energy-autocorrelation function which contribute to the field-parallel enhancement of heat conduction in strongly coupled plasmas. The investigation is based on first-principle molecular dynamics simulations.

© 2016 WILEY-VCH Verlag GmbH & Co. KGaA, Weinheim

1 Introduction

Strongly coupled plasmas (SCPs)—in which the interaction energy of neighboring particles is larger than the thermal energy—are abundant in nature and experiments. Experimental realizations include dusty plasmas [1, 2], ultracold plasmas [3], and trapped ions [4]. Studies of these systems promise insight into naturally occurring SCPs such as white dwarf stars [5], the neutron star atmosphere [5, 6] or other, less accessible experiments such as laser-generated warm dense matter [7] or the strongly coupled liner remnants in Magnetized Liner Inertial Fusion (MagLif) experiments [8].

In many of these SCPs, strong magnetic fields influence the dynamics of the particles. Such scenarios occur, e.g., in magnetic neutron stars [9, 10], MagLif experiments, or in laser fusion setups via self-generated strong magnetic fields [11]. The magnetization of dusty plasmas is an ongoing challenge [12] which is supplemented by efforts to imprint an effective magnetic field on the dust particle dynamics by setting the dusty plasma into rotation [13–15].

Consequently, magnetized SCPs have drawn much attention in the past and have been investigated, e.g., through numerical simulations [16–24], analytical modelling [25–27], and kinetic theory [28–31]. The present authors have recently presented a study of the thermal conductivity of magnetized SCPs through equilibrium simulations [32], supplementing similar simulations of unmagnetized SCPs [33–38] and studies of weakly coupled magnetized plasmas, e.g., Refs. [39, 40].

In this article, we make use of the microscopic data obtained from equilibrium simulations to investigate the energy-autocorrelation function (EACF) [36, 41]. The EACF is related to the thermal conductivity via the Green-Kubo formula (see Eq. (3) below), i.e., the time-integral over the EACF converges to the thermal conductivity coefficient. By considering the EACF and its dependence on the magnetic field, one obtains additional insight into the microscopic processes responsible for the (macroscopic) response of the plasma to a temperature gradient. The remainder of this paper is organized as follows: In Sec. 2 we introduce the EACF and its calculation from molecular dynamics (MD) simulation. Section 3 contains details of the model used for the calculation and the MD simulation itself. Section 4 presents results for the EACF of unmagnetized and magnetized SCPs and identifies the main processes responsible for the heat transport. We conclude in Sec. 5.

* Corresponding author. E-mail: ott@theo-physik.uni-kiel.de

2 Energy Autocorrelation Function

The microscopic energy flux in a plasma is given by the the Irving-Kirkwood formula [41, 42],

$$\mathbf{j} = \sum_{i=1}^N \mathbf{v}_i \left[\frac{1}{2} m |\mathbf{v}_i|^2 + \frac{1}{2} \sum_{j \neq i}^N \phi(r_{ij}) \right] + \frac{1}{2} \sum_{i=1}^N \sum_{j \neq i}^N (\mathbf{r}_{ij} \cdot \mathbf{v}_i) \mathbf{F}_{ij}, \quad (1)$$

$$= \mathbf{j}^{\text{kin}} + \mathbf{j}^{\text{pot}} + \mathbf{j}^{\text{coll}} \quad (2)$$

which comprises a kinetic, a potential, and a collision contribution (first, second, and last term, respectively). The first two contributions represent the transport of energy associated with the bodily movement of particles, while the collision term represents the transfer of momentum and energy mediated by the mutual interaction of the particles.

The energy flux (1) is a collective property of the whole plasma and is, in itself, of little interest, since it is a rapidly fluctuating quantity. The autocorrelation function of the energy flux (the EACF), however, provides insight into the time scales of heat transfer in the system. By means of the decomposition (2), one can, in addition, ascertain the dominant mode of energy transfer, e.g., as a function of the temperature or the magnetic field.

The integral over the EACF is related to the heat conductivity of the plasma via the well-known Green-Kubo formula [41], i.e.,

$$\lambda_{\mu\nu} = \frac{1}{V k_B T^2} \int_0^\infty C_{\mu\nu}(t) dt, \quad C_{\mu\nu} = \langle j_\mu(t) j_\nu(0) \rangle \quad (3)$$

where V is the total volume of the system and T its temperature. Although the integral in Eq. (3) extends to infinity, it is, in practice, truncated at a finite time after convergence has been observed.

In a magnetized system, the heat conductivity tensor $\lambda_{\mu\nu}$ and, accordingly, the EACF tensor $C_{\mu\nu} = \langle j_\mu(t) j_\nu(0) \rangle$ consist of three independent components, e.g., $C_\perp = C_{xx} = C_{yy}$, $C_\parallel = C_{zz}$, and $C_\times = C_{xy} = -C_{yx}$, assuming $\vec{B} \parallel \hat{e}_z$. Here, we consider only the diagonal components of the EACF tensor, that is, the field-parallel (C_\parallel) and the cross-field (C_\perp) heat transfer. These two components are further decomposed into six contributions, e.g.,

$$C_\perp = C_\perp^{\text{kk}} + C_\perp^{\text{pp}} + C_\perp^{\text{cc}} + 2C_\perp^{\text{kp}} + 2C_\perp^{\text{kc}} + 2C_\perp^{\text{pc}},$$

which are the direct and cross-correlation terms resulting from insertion of Eq. (2) into Eq. (3), i.e., kinetic-kinetic, potential-potential, and so forth.

3 Methods and Simulation Details

Our interest is in the properties of the EACF tensor in a strongly coupled plasma, both in the presence of a strong magnetic field and in the unmagnetized case. To isolate the most fundamental effects, and because a fully self-consistent simulation of a strongly coupled plasma is not feasible, we consider the paradigmatic model of a (screened) one-component plasma (OCP). In this model, N particles with uniform mass m and charge Q interact via a Debye-Hückel potential

$$\phi(r) = Q^2/r \times \exp(-r/\Lambda) \quad (4)$$

with screening length $\Lambda = a/\kappa$, where κ is the dimensionless screening parameter and a is the Wigner-Seitz radius. To characterize the OCP, it suffices to give the screening parameter κ (we consider $\kappa = 2$ throughout this work) and the coupling parameter $\Gamma = Q^2/(k_B T a)$ and to specify the field strength as $\beta = \omega_c/\omega_p$, in which $\omega_p = [4\pi Q^2 n/m]^{1/2}$ is the plasma frequency and $\omega_c = qB/(mc)$ the cyclotron frequency.

We solve the equations of motion for $N = 8192$ particles in periodic boundary conditions via molecular dynamics simulation, incorporating the magnetic field into the integration scheme [43, 44]. All data points are obtained from simulations spanning $\omega_p t = 1.25 \times 10^7$, divided into 50 independent runs. The resulting EACF is calculated from Eq. (1) for each simulation and averaged over all runs.

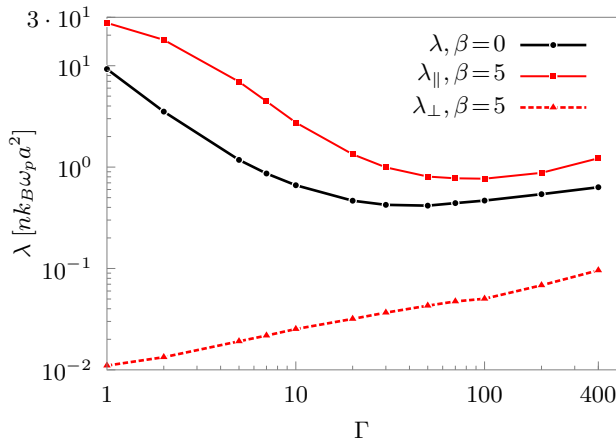


Fig. 1 Heat conductivity as a function of the coupling strength in an unmagnetized system ($\beta = 0$, middle curve) and in field-parallel and cross-field direction in a strongly magnetized system ($\beta = 5$, upper and lower curve, respectively). Data reproduced from Ref. [32].

4 Results

Before considering the EACF, we recall some main results from our calculation of the heat conductivity in strongly coupled OCPs [32] for $\kappa = 2$, see Fig. 1. The heat conductivity is a non-monotonic function of the coupling strength in the unmagnetized case, varying over more than one order of magnitude from $\Gamma = 1$ to $\Gamma = 400$, close to the crystallization point. The minimum occurs around $\Gamma = 35$. As in a weakly coupled plasma ($\Gamma \ll 1$), a magnetic field strongly reduces the ability of the plasma to transport heat perpendicular to the field. This reduction can amount to orders of magnitude (see bottom curve of Fig. 1) and is strongest for small Γ . For field-parallel transport, on the other hand, strong coupling effects massively change the behavior of the magnetized plasma. While for weakly coupled plasmas ($\Gamma \ll 1$), the heat transport is independent of the B -field [39], it can be strongly enhanced in the case of strong coupling (see upper curve in Fig. 1).

We have quantified and explained these effects in detail in Ref. [32]. Here, we concentrate on the properties of the EACF itself, i.e., the integrand of the Green-Kubo formula. This will allow us to identify the time scales involved in the reduction and enhancement of the heat conductivity as well as the relative contributions according to Eq. (2).

4.1 Unmagnetized Systems

We begin by considering the unmagnetized system at three representative values for the coupling, $\Gamma = 5, 30, 300$, corresponding to values at the falling and rising flanks and the minimum in $\lambda(\Gamma)$ (see Fig. 1). In Fig. 2, the six components of the EACF and their sum, i.e., the total EACF, are shown. For $\Gamma = 5$, all autocorrelation functions are smoothly decaying functions, with the exception of the kinetic-potential and the kinetic-collisional cross terms, which only contribute at time delays of more than one plasma cycle ω_p^{-1} . The total EACF is dominated by the kinetic contribution, whereas collisional and potential contributions are only minor, as is expected for a comparably weakly coupled system. After a time of $30\omega_p^{-1}$, the integral of the EACF, i.e., the total thermal conductivity, converges to its final value (see bottom part of Fig. 2). The contribution of the direct kinetic correlation term is larger than 80%.

At $\Gamma = 30$, the EACF is an oscillatory function due to the increased interparticle coupling. This is mainly driven by the increase of the relative contribution of the collisional correlation function, which reflects the increasingly caged motion of the particles. In light of the finite integration time required for the Green-Kubo formula (3), it is especially noteworthy that the oscillation of the EACF extends to negative values around $10\omega_p^{-1}$. This leads to the formation of an associated plateau in the integrated EACF which could be misinterpreted as convergence.¹ At this intermediate coupling, the contributions of direct kinetic and collisional correlations are of comparable magnitude, and, in fact, their contrary dependence on Γ is the reason for the formation of a minimum in $\lambda(\Gamma)$.

¹ A common method for determining the endpoint of the integration in Eq. (3) is to identify it with the first zero crossing of the EACF.

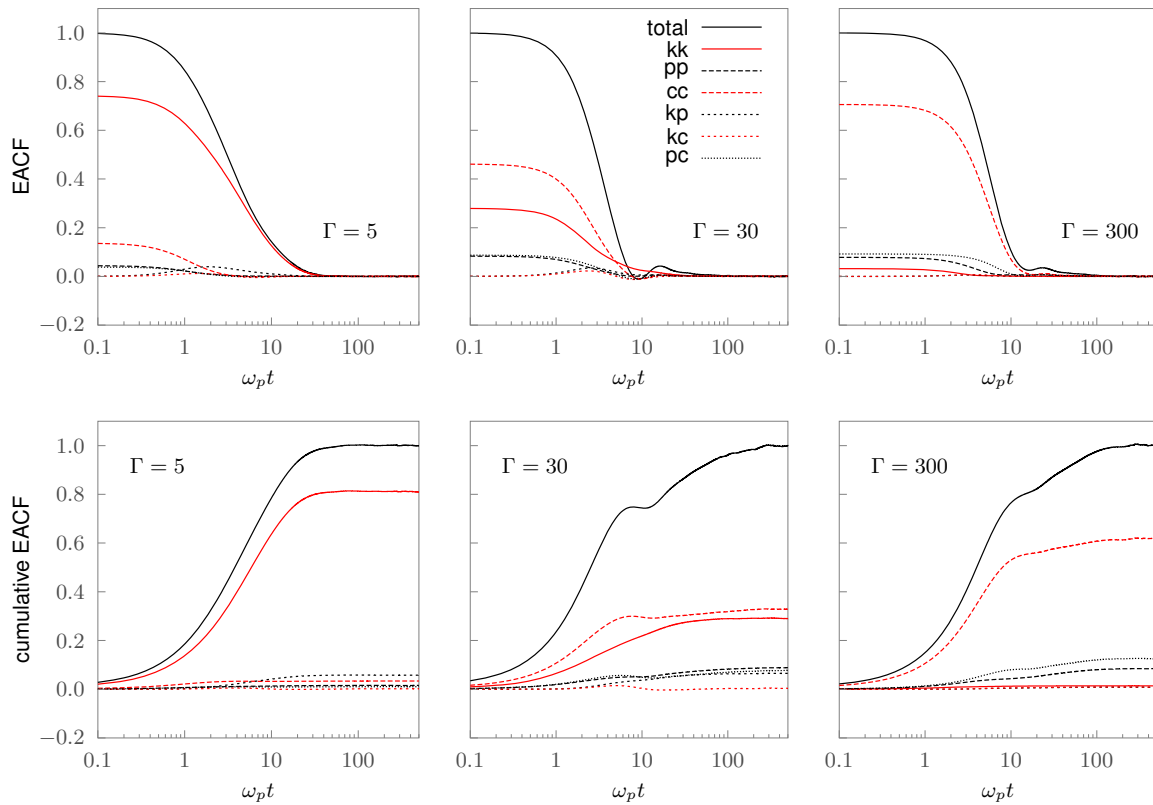


Fig. 2 Results for three unmagnetized systems at weak to strong coupling. **Top:** Total (normalized) EACF and its decomposition into six contributions. **Bottom:** The corresponding running integral of the EACF normalized to converge to unity. Note the difference in the leading contribution for weak and strong coupling as well as the occurrence of negative portions in the EACF for $\Gamma = 30$ and the corresponding formation of a plateau in the integrated EACF (middle column).

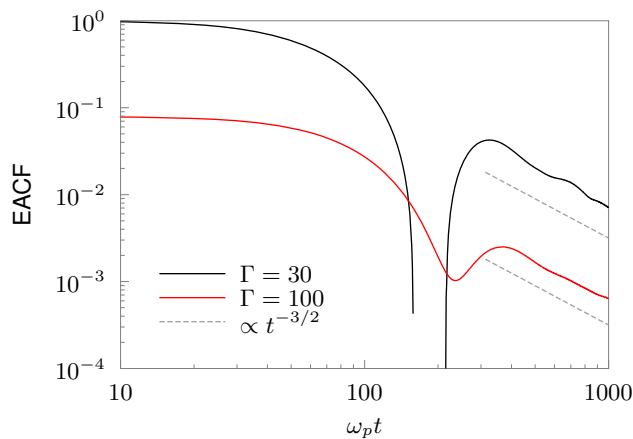


Fig. 3 The EACF of two unmagnetized systems at $\Gamma = 30$ and $\Gamma = 100$, normalized to the EACF for $\Gamma = 30$ at $t = 0$. The decay of the EACF follows $t^{-3/2}$ in both cases, indicating the existence of a long-time tail.

At the other end of the liquid coupling range, at $\Gamma = 300$, the collisional mode is dominant since the particles are arranged in an almost stationary lattice-like configuration. Transport of heat via the direct kinetic channel is suppressed, but the slowly changing particle landscape is reflected in the contribution of the potential term, which is comparable to the collisional-potential cross term. Convergence for $\Gamma = 30$ and $\Gamma = 300$ is considerably slower than in the more weakly coupled system and is only observed at times larger than $100\omega_p^{-1}$.

Lastly, we consider the decay rate of the EACF at long time delays, Fig. 3. The form of this decay is of considerable interest for fundamental questions such as the existence of transport coefficients in lower dimensions [36, 45, 46]. For $\Gamma = 30$ and 300 , we find evidence for the existence of an algebraic decay proportional to $t^{-D/2}$, where $D = 3$ is the dimensionality of the system, the so-called long-time tail [47–49]. This is in agreement with earlier simulations for two-dimensional systems [36] which provided evidence for a $1/t$ -decay for warm systems, possibly excluding the existence of a heat conductivity coefficient in two dimensions.

4.2 Magnetized Systems

For the magnetized system, we restrict the discussion to the field-parallel component of the EACF tensor, since the suppression of the cross-field transport, at high enough magnetic field, is very efficient and the energy flux perpendicular to the field is therefore negligible.

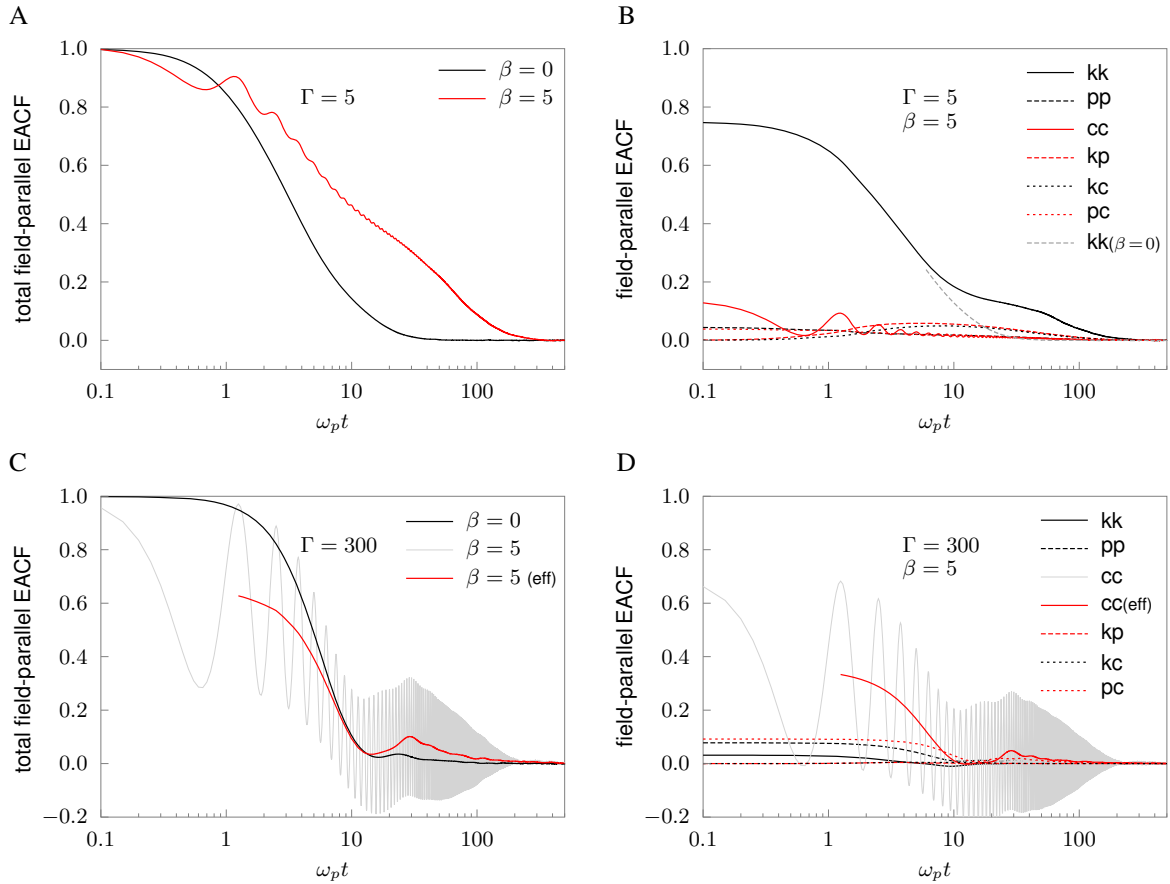


Fig. 4 **A, C:** The (normalized) field-parallel EACF at $\beta = 0$ and $\beta = 5$ for $\Gamma = 5$ and $\Gamma = 300$. **B, D:** The corresponding contributions to the total field-parallel EACF at $\beta = 5$. In **C** and **D**, the effective contribution of the oscillatory EACF to the Green-Kubo integral is shown by the strong red line. In **B**, the dashed grey line shows the direct kinetic EACF of an unmagnetized system. Note the logarithmic scaling of the time axis and the resulting distortion of area sizes.

First, consider a comparably weakly coupled system ($\Gamma = 5$) in which unmagnetized transport is dominated by the kinetic contribution and, at strong magnetic fields, there is a substantial enhancement of the heat conductivity. Figure 4A shows the temporal evolution of the total EACF at $\beta = 0$ and $\beta = 5$. From these data, we conclude that the increasingly effective field-parallel transport is driven by an enhanced persistence of the heat flux at time scales between $t\omega_p = 10 \dots 200$. As Fig. 4B shows, this persistence in turn can be largely attributed to the formation of a shoulder-like feature in the direct kinetic term of the EACF (the grey dashed line in Fig. 4B shows the corresponding direct kinetic term at zero magnetic field). Additional contributions arise from the kinetic-potential and the kinetic-collisional cross terms at early times. We conclude that the magnetic field enhances

kinetic energy retention in field-parallel direction for surprisingly long times and attribute this to the decreased mutual interaction with (perpendicularly situated) neighboring particles due to the tightly-wound Larmor radii at large fields.

We now turn to the opposite extreme of a system with collisionally dominated transport, $\Gamma = 300$. Since the EACF is highly oscillatory at $\beta = 5$, we calculate the effective contribution to the Green-Kubo integral by averaging the upper and lower hull curves. These data are plotted in Fig. 4C and D alongside the actual EACF. As these data show, the enhancement of field-parallel transport originates primarily from the growth of the first oscillation in the direct collision EACF contribution and occurs at time scales of $t\omega_p = 20 \dots 100$. This indicates that the interaction times of particles undergoing a collision are much prolonged. We attribute this to the decreased mobility of particles in the field-perpendicular direction which prevents a rapid repulsion of interacting particles.

5 Conclusion

In summary, we have calculated the energy autocorrelation function (EACF) in a screened one-component plasma. The present results supplement those of Ref. [32] in characterizing the heat conduction process in strongly coupled plasmas and the processes leading to the field-parallel enhancement of heat transport by a magnetic field. They also represent the first detailed study of the composition of the total EACF from its six constituent parts and their functional forms.

In unmagnetized plasmas, there exist different regimes of Γ , in which either kinetic (small Γ) or collisional (large Γ) transport channels dominate. At intermediate coupling near the onset of caging ($\Gamma = 30$), the EACF can become negative at intermediate time scales and is dominated in equal parts by the kinetic and collisional transport channel. For strongly magnetized plasma, we have investigated the surprising result that the field-parallel heat conductivity is enhanced over the unmagnetized case. By observing the time evolution of the EACF in a magnetized system, we have identified the dominant channels and the time scales on which the enhanced heat flux persistence occurs.

Acknowledgements This work was supported by the Deutsche Forschungsgemeinschaft via SFB-TR 24 project A7, grant shp00014 at the North-German Supercomputing Alliance (HLRN), and grant K-105476 of the Hungarian Fund for Scientific Research (OTKA).

References

- [1] A. Ivlev, G. Morfill, H. Löwen, and C. Royall, *Complex Plasmas and Colloidal Dispersions: Particle-resolved Studies of Classical Liquids and Solids*, Series in soft condensed matter (World Scientific Publishing Company, Incorporated, 2012).
- [2] M. Bonitz, C. Henning, and D. Block, *Rep. Prog. Phys.* **73**, 066501 (2010).
- [3] S.L. Rolston, *Physics* **1**, 2 (2008).
- [4] D.H.E. Dubin and T.M. O'Neil, *Rev. Mod. Phys.* **71**, 87 (1999).
- [5] S. Shapiro and S. Teukolsky, *Black holes, white dwarfs, and neutron stars: The physics of compact objects* (Wiley, New York, 1983).
- [6] A.Y. Potekhin, *Physics-Uspekhi* **53**, 1235 (2010).
- [7] M. Koenig, A. Benuzzi-Mounaix, A. Ravasio, T. Vinci, N. Ozaki, S. Lepape, D. Batani, G. Huser, T. Hall, D. Hicks, A. MacKinnon, P. Patel, H.S. Park, T. Boehly, M. Borghesi, S. Kar, and L. Romagnani, *Plasma Phys. Controlled Fusion* **47**, B441 (2005).
- [8] M.R. Gomez et al., *Phys. Rev. Lett.* **113**, 155003 (2014).
- [9] D. Page, U. Geppert, and M. Küker, *Astrophys. Space Sci.* **308**, 403 (2007).
- [10] A. Chugunov and P. Haensel, *Mon Not R Astron Soc.* **381**, 1143 (2007).
- [11] J.R. Rygg, F.H. Sguin, C.K. Li, J.A. Frenje, M.J.E. Manuel, R.D. Petrasso, R. Betti, J.A. Delettrez, O.V. Gotchev, J.P. Knauer, D.D. Meyerhofer, F.J. Marshall, C. Stoeckl, and W. Theobald, *Science* **319**, 1223 (2008).
- [12] E. Thomas, R.L. Merlino, and M. Rosenberg, *Plasma Phys. Controlled Fusion* **54**, 124034 (2012).
- [13] P. Hartmann, Z. Donkó, T. Ott, H. Kählert, and M. Bonitz, *Phys. Rev. Lett.* **111**, 155002 (2013).
- [14] M. Bonitz, H. Kählert, T. Ott, and H. Löwen, *Plasma Sources Sci T* **22**, 015007 (2013).
- [15] H. Kählert, J. Carstensen, M. Bonitz, H. Löwen, F. Greiner, and A. Piel, *Phys. Rev. Lett.* **109**, 155003 (2012).
- [16] K.N. Dzhamagulova, R.U. Masheeva, T.S. Ramazanov, and Z. Donkó, *Phys. Rev. E* **89**, 033104 (2014).

- [17] L.J. Hou, Z.L. Mišković, A. Piel, and M.S. Murillo, *Phys. Rev. E* **79**, 046412 (2009).
- [18] M. Bonitz, Z. Donkó, T. Ott, H. Kählert, and P. Hartmann, *Phys. Rev. Lett.* **105**, 055002 (2010).
- [19] T. Ott, M. Bonitz, P. Hartmann, and Z. Donkó, *Phys. Rev. E* **83**, 046403 (2011).
- [20] T. Ott, H. Löwen, and M. Bonitz, *Phys. Rev. Lett.* **111**, 065001 (2013).
- [21] B. Bernu, *J. Phys. Lett. Paris* **42**, 253 (1981).
- [22] T. Ott and M. Bonitz, *Phys. Rev. Lett.* **107**, 135003 (2011).
- [23] Y. Feng, J. Goree, B. Liu, T.P. Intrator, and M.S. Murillo, *Phys. Rev. E* **90**, 013105 (2014).
- [24] T. Ott, H. Löwen, and M. Bonitz, *Phys. Rev. E* **89**, 013105 (2014).
- [25] T. Ott, H. Kählert, A. Reynolds, and M. Bonitz, *Phys. Rev. Lett.* **108**, 255002 (2012).
- [26] H. Kählert, T. Ott, A. Reynolds, G.J. Kalman, and M. Bonitz, *Phys. Plasmas* **20**, 057301 (2013).
- [27] T. Ott, D.A. Baiko, H. Kählert, and M. Bonitz, *Phys. Rev. E* **87**, 043102 (2013).
- [28] L. Suttorp and J. Cohen, *Physica A* **133**, 370 (1985).
- [29] L. Suttorp and A. Schoolderman, *Physica A* **141**, 1 (1987).
- [30] L.G. Suttorp and J.S. Cohen, *Physica A* **123**, 560 (1984).
- [31] J.S. Cohen and L.G. Suttorp, *Physica A* **126**, 308 (1984).
- [32] T. Ott, M. Bonitz, and Z. Donkó, *Phys. Rev. E* **92**, 063105 (2015).
- [33] Z. Donkó and B. Nyíri, *Phys. Plasmas* **7**, 45 (2000).
- [34] G. Salin and J.M. Caillol, *Phys. Rev. Lett.* **88**, 065002 (2002).
- [35] Z. Donkó and P. Hartmann, *Phys. Rev. E* **69**, 016405 (2004).
- [36] Z. Donkó, J. Goree, P. Hartmann, and B. Liu, *Phys. Rev. E* **79**, 026401 (2009).
- [37] Y.V. Khrustalyov and O.S. Vaulina, *Phys. Rev. E* **85**, 046405 (2012).
- [38] G. Kudelis, H. Thomsen, and M. Bonitz, *Phys. Plasmas* **20**, 073701 (2013).
- [39] S.I. Braginskii, *Transport Processes in a Plasma*, Reviews of Plasma Physics, Vol.1 (Consultants Bureau, New York, 1965).
- [40] R. Balescu, *Transport processes in plasmas*, Vol. 1: Classical Transport (North-Holland Publishing Company, Amsterdam, 1988).
- [41] J. Hansen and I. McDonald, *Theory of Simple Liquids* (Academic Press, London, 2006).
- [42] J.H. Irving and J.G. Kirkwood, *J. Chem. Phys.* **18**, 817 (1950).
- [43] Q. Spreiter and M. Walter, *J. Comput. Phys.* **152**, 102 (1999).
- [44] S.A. Chin, *Phys. Rev. E* **77**, 066401 (2008).
- [45] T. Ott and M. Bonitz, *Phys. Rev. Lett.* **103**, 195001 (2009).
- [46] T. Ott, M. Bonitz, Z. Donkó, and P. Hartmann, *Phys. Rev. E* **78**, 026409 (2008).
- [47] B. Alder and T. Wainwright, *Phys. Rev. A* **1**, 18 (1970).
- [48] K. Kawasaki, *Phys. Lett. A* **32** (1970).
- [49] M. Isobe, *Phys. Rev. E* **77**, 021201 (2008).